

Lead isotopic analysis of infant bone tissue dating from the Roman era via multicollector ICP–mass spectrometry

David De Muynck · Christophe Cloquet ·
Elisabeth Smits · Frederik A. de Wolff ·
Ghyslaine Quitté · Luc Moens · Frank Vanhaecke

Received: 7 July 2007 / Revised: 1 October 2007 / Accepted: 5 October 2007 / Published online: 30 October 2007
© Springer-Verlag 2007

Abstract Archaeological samples originating from a cemetery of a Roman settlement, *Pretorium Agrippinae* (1st–3rd century A.D.), excavated near Valkenburg (The Netherlands) have been subjected to Pb isotopic analysis. The set of samples analysed consisted of infant bone tissue and possible sources of bone lead, such as the surrounding soil, garum, and lead objects (e.g., water pipes). After sample digestion with quantitative Pb recovery and subsequent quantitative and pure isolation of lead, the Pb isotopic composition was determined via multicollector ICP–mass spectrometry. The Pb isotope ratio results allowed distinction of three groups: bone, soil, and lead objects + garum. The $^{208}\text{Pb}/^{206}\text{Pb}$ ratio ranges were between 2.059 and 2.081 for the soils, between 2.067 and 2.085 for the bones, and between 2.087 and 2.088 for the lead objects. The garum sample is characterised by a $^{208}\text{Pb}/^{206}\text{Pb}$ ratio of 2.085. The bone group is situated on the mixing line between the soil and lead object groups,

allowing the statement that diagenesis is not the main cause of the Pb found in the bones.

Keywords Multicollector ICP–MS · Pb isotopic analysis · Bone tissue · Soil · Roman era

Introduction

Among the mass spectrometric techniques developed in the 20th century, thermal ionization–mass spectrometry (TI–MS) has been established as the reference technique for high-precision isotope ratio analysis of the heavier elements [1]. However, since its commercial introduction in 1983, inductively coupled plasma–mass spectrometry (ICP–MS) has gained growing importance as a technique for trace element analysis and isotope ratio determination. ICP–MS offers important benefits over TI–MS (e.g., the continuous nebulisation of sample solution into an ion source at atmospheric pressure, the higher sample throughput, and the high ionisation efficiency of the ICP) [2, 3]. Modern multicollector ICP–mass spectrometry (MC–ICP–MS) combines these benefits with excellent isotope ratio precision [4–7]. Moreover, in present multicollector ICP–MS instrumentation, the double-focusing sector-field mass spectrometer can be operated under so-called pseudo–high-resolution conditions, permitting many spectral interferences to be avoided, while at the same time the flat-topped peak shapes are preserved, thus maintaining an excellent isotope ratio precision [8]. In MC–ICP–MS, it has been observed that the matrix strongly affects mass discrimination [9, 10], and an adequate correction is required to obtain accurate results [11, 12]. When mass discrimination correction is performed using an external standard with a known isotopic compo-

D. De Muynck (✉) · C. Cloquet · L. Moens · F. Vanhaecke
Department of Analytical Chemistry, Ghent University,
Krijgslaan 281–S12,
9000 Ghent, Belgium
e-mail: David.DeMuynck@UGent.be

E. Smits
Amsterdam Archaeological Center, University of Amsterdam,
Turfdraggsterpad 9,
1012 XT Amsterdam, The Netherlands

F. A. de Wolff
Toxicology Laboratory, Leiden University Medical Center,
L1-P, P.O. Box 9600, 2300 RC Leiden, The Netherlands

G. Quitté
Institute for Isotope Geomistry and Mineral Resources,
ETH Zürich, Clausiusstrasse 25,
8092 Zürich, Switzerland

sition, the matrix composition of the standard has to be similar to that of the sample, and even the analyte concentrations in sample and standard have to be similar [13, 14]. Consequently, isolation of the target element from the matrix is required in order to obtain reliable results via multicollector ICP–MS.

Lead is a widely used metal (e.g., in ancient times for manufacturing trays and kitchen utensils, in more recent times for constructing electric batteries for vehicles, as an additive in gasoline, in paints), but at the same time, it is a versatile, insidious, and persistent poison. Metallic lead has been in the human environment for over 5000 years [15]. Effects of lead toxicity, which manifests itself by, e.g., anaemia and coma, had already been described in ancient times by Hippocrates in 370 B.C. [15]. Many more negative effects of lead are known at present. Organic (tetraethyl) lead affects the nervous system [16], while inorganic lead acts on different body functions and systems, e.g., heme synthesis [17], reproduction [18], nervous system, and kidneys [19]. From epidemiological studies, inconclusive evidence has been found as to a causal relation between lead exposure and the incidence of cancer. At present, there are insufficient data for suggesting that lead compounds are carcinogenic to humans [20]. More detailed information on lead toxicity can be found elsewhere, e.g., Gidlow [16] and Papanikolaou et al. [21].

Lead can enter the body via different pathways: by ingestion through the intestines, by inhalation through the lungs, by direct swallowing, and through the skin [15]. Inorganic lead absorption takes place throughout the respiratory and gastrointestinal tracts, while organic (tetraethyl) lead can be absorbed by the skin. After lead exposure, the lead is absorbed into the blood and transported to other tissues. Lead predominantly accumulates in three compartments: blood, soft tissues, and bone [22]. Approximately 99% of the lead in blood is found in the erythrocytes, leaving about 1% in the plasma. More than 95% of lead is deposited in skeletal bone as insoluble phosphate [22]. In adults, 80 to 95% of the body's lead burden is found in the skeleton, for children, this is only 73%. Lead has an estimated half-life of 20 to 30 years in bone tissue [21, 23] and its concentration in bone and teeth increases as a function of age. In general, lead is excreted extremely slowly from the body. Its biological half-life is estimated at 10 years [15].

Due to the radioactive decay of the naturally occurring and long-lived radionuclides ^{232}Th , ^{235}U , and ^{238}U into ^{208}Pb , ^{207}Pb , and ^{206}Pb , respectively, lead shows quite a large variation in isotopic composition [24]. This makes Pb isotopic analysis a powerful tool for studies in various fields, e.g., dating studies [25], environmental studies [26, 27], and archaeology [28–30].

The results reported in the current paper stem from a multi-disciplinary (geochemical, archaeological, and tox-

icological) study, investigating high infant mortality in the Roman era. It is well known that the Romans used lead for many applications (e.g., water pipes, Pb salts for food conservation, etc. [31]), and the possibility of a link between the decline of the Roman Empire and lead poisoning has been expressed earlier [32, 33]. Approximately 26% of Roman children died before the age of fourteen, while approximately 14% even died in the first year of life. To investigate the cause of this high infant mortality, self-evidently, only the skeletal remains are accessible. In paleopathology, the cause of death can seldom be detected from the bone material. In this case however, the availability of infant remains in association with existing theories of the abundant use of lead during the Roman period instigated a chemical/toxicological study of the infant bones to discover whether the ingestion of lead during pregnancy might have been the origin of or contributed to the death of these infants. The samples subject to investigation consist of infant bone tissue and possible sources of bone lead, such as the surrounding soil, garum, and lead objects, all dating from the Roman era. The goal of the study reported here is to clarify whether the lead which is now present in the bone tissue has entered the bone throughout the past 2000 years via diagenesis from the soil, or via another mechanism.

Experimental

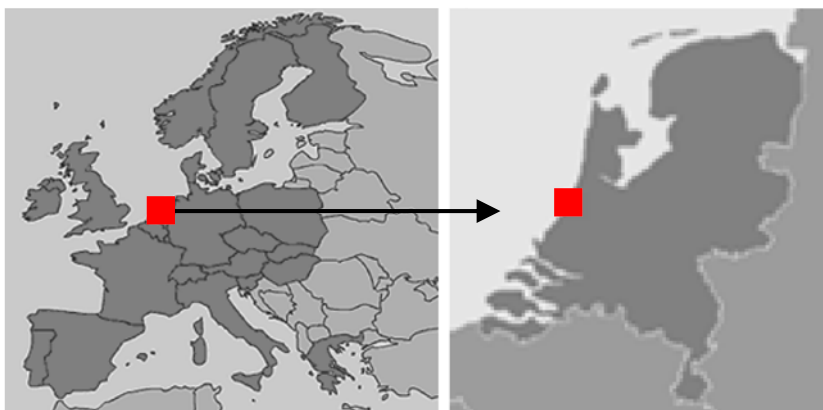
Description of the sampling site and the samples

The archaeological samples investigated in this work originate from the cemetery of a Roman settlement, and were excavated near Valkenburg, situated on the Southern shore of the river Rhine, in the West of The Netherlands (Fig. 1). This river marked the Northern frontier in this part of the Roman Empire. This frontier was defended by many military fortresses connected by the Roman road. In the period 1st–3rd century A.D., several military forces were settled in a fortress at Valkenburg, at that time known as *Pretorium Agrippinae*. In the vicinity, archaeological excavations uncovered the remains of a civilian settlement and a large cemetery [34–36]. This cemetery yielded many cremation graves, as older children and adults were customarily cremated in Roman days. However, the Roman rule also stipulated that young infants without teeth should be buried instead of cremated, as described by Plinius [37].

In most Roman cemeteries, the remains of very young infants (buried in inhumation graves) are mostly absent because:

1. the fragility of the remains and the soil conditions often did not favour preservation of bone tissue; and

Fig. 1 Geographical location of Valkenburg, situated in The Netherlands, Europe



2. these small and fragile bones are easily missed as a result of the archaeological excavation methods typically used in the field.

At Valkenburg however, an exceptionally high number of infant graves were discovered, even providing a fair insight into the percentage of infant graves in relation to the total cemetery population. The excavations at the grave field resulted in the discovery of the remains of a total of 683 individuals in 520 cremation graves and 134 inhumation graves. The age and/or sex were determined for 503 individuals. In 176 graves—81 cremation graves and 95 inhumation graves—skeletal remains of children between 0 and 14 years of age were discovered. It was established that 84 of the 95 inhumed infant skeletons found stemmed from infants younger than 1 year [38]. These remains are the subject of investigation in this study.

A set of 22 bone tissue samples, taken throughout the entire excavation site, was subject to Pb isotopic analysis. The bone samples were taken from femuræ from deceased and stillborn Roman infants of which, at present, the sex is not known. The cortical bone tissue (hard outer tissue) was sampled. This area is free of foreign material—and thus provides the most accurate results—in contrast with trabecular bone (inner tissue in which the bone metabolism occurs), which contains excessive amounts of intruded soil particles and hence, is less reliable [38]. Every bone sample was accompanied by a sample from the surrounding soil from which the bone was excavated, thus leading to 22 pairs of bone tissue and soil. Only small sample amounts (≤ 1 g) of bone and soil were available. Possible sources of bone lead, next to soil, consisted of five lead objects (e.g., water pipes) and one sample of fish bones. These fish bones originate from a large earthenware bowl, which was excavated at the site and which was filled with hundreds of fish bones. This find was interpreted as the remains of the well-known Roman dish, *garum*, a fermented fish sauce enriched with *sapa*, a substance with a high lead content and added to many recipes because of its sweet taste and preservative

character. In the following text, this fish bone sample will always be referred to as *garum*.

Sample preparation

Pro analysi nitric acid (14 mol L^{-1}) and hydrochloric acid (12 mol L^{-1}) (Panreac, Spain) were further purified by subboiling distillation in quartz equipment. Hydrofluoric acid (22 mol L^{-1} , *intra-analysed*) and perchloric acid (10 mol L^{-1} , *intra-analysed*) were bought from J.T. Baker Chemicals, The Netherlands, and *pro analysi* hydrogen peroxide (10 mol L^{-1}) was purchased from Merck, Germany. Ultrapure water of resistivity $>18 \text{ M}\Omega \text{ cm}$ was obtained from a Milli-Q system (Millipore, USA) and used throughout this work for preparing dilutions. *Pro analysi* ammonium oxalate, $(\text{NH}_4)_2\text{C}_2\text{O}_4 \cdot 2\text{H}_2\text{O}$, was purchased from UCB, Belgium.

The lead objects were dissolved in $1.4 \text{ mol L}^{-1} \text{ HNO}_3$ on a hotplate, while the bone, *garum*, and soil samples were digested by microwave-assisted acid digestion using a suitable combination of acids (bone and *garum*: $\text{HNO}_3 + \text{HCl}$, soil: $\text{HNO}_3 + \text{HCl} + \text{HF} + \text{HClO}_4$), followed by evaporation on a hotplate at 105°C and uptake of the residue in concentrated HNO_3 . After this digestion step, the Pb was isolated from its matrix by means of an extraction chromatographic separation, using a column containing a commercially available lead-selective crown ether (Eichrom Technologies, France). The digestion and isolation processes result in a quantitative Pb recovery, and a pure Pb fraction is obtained after the isolation procedure. A detailed description of the sample digestion and Pb isolation procedure can be found in De Muynck et al. [39].

After the isolation procedure, the Pb fraction of the sample was present in a $0.05 \text{ mol L}^{-1} (\text{NH}_4)_2\text{C}_2\text{O}_4$ solution. In order to remove the $(\text{NH}_4)_2\text{C}_2\text{O}_4$ present, an aliquot of the sample was evaporated to dryness followed by addition of $1 \text{ mL } 14 \text{ mol L}^{-1} \text{ HNO}_3 + 1 \text{ mL } 10 \text{ mol L}^{-1} \text{ H}_2\text{O}_2$. After a few hours, the sample was evaporated to dryness again. Finally, the residue was taken up in $0.5 \text{ mol L}^{-1} \text{ HNO}_3 + 0.22 \text{ mol L}^{-1} \text{ HF}$, hereby adjusting the Pb concentration to $\sim 30 \text{ ng mL}^{-1}$.

Isotope ratio measurement and mass discrimination correction

The samples reported in this study were measured on a Nu Plasma multicollector ICP–mass spectrometer [40]. The sample introduction system consisted of an Aridus desolvating system. Data acquisition was done in 60 cycles of 5 s integration, grouped in blocks of 20 cycles. Outliers were removed by the software after a 2 *s* test. All isotope ratio measurements were carried out by static multicollection with Faraday cups. The detectors Low 4, Low 3, Low 2, Low 1, Axial, High 1 and High 2 were used to record the ion intensities of ^{202}Hg , ^{203}Tl , ^{204}Pb , ^{205}Tl , ^{206}Pb , ^{207}Pb , and ^{208}Pb , respectively. The intensity measured at $m/z=204$ was corrected for ^{204}Hg interference using a $^{204}\text{Hg}/^{202}\text{Hg}$ ratio of 0.229. The $^{204}\text{Hg}/^{204}\text{Pb}$ ratio turned out to be negligible (average: 4×10^{-5}).

The samples were measured using both sample-standard bracketing with a solution of NIST SRM 981 Common Lead as isotopic standard, and Tl external normalization. For both samples and standards, the Pb concentration was $\sim 30 \text{ ng mL}^{-1}$, and Tl (NIST SRM 997) was added at a concentration of $\sim 7.5 \text{ ng mL}^{-1}$. Mass discrimination correction was performed via Russell's exponential law as described by White et al. [41]. Russell's equation was used to calculate the mass discrimination factors β_{Tl} (using the certified NIST SRM 997 $^{205}\text{Tl}/^{203}\text{Tl}$ ratio of 2.38714) and β_{Pb} (using the accepted values for NIST SRM 981 as given by Galer and Abouchami [42], $^{208}\text{Pb}/^{206}\text{Pb}=2.16771$) for the standards. Plotting β_{Pb} versus β_{Tl} for the measurements of the standard solution carried out throughout the entire session resulted in a linear relationship. This relationship was used to calculate the mass discrimination factor β_{Pb} for every unknown sample from the corresponding experimentally determined β_{Tl} value for that sample, and the mass discrimination factor β_{Pb} was subsequently used to calculate the true Pb isotope ratio. Blank Pb signals were negligible compared to the Pb signals encountered for samples and standards ($<0.1\%$). Within the external precision, the average Pb isotope ratios obtained for NIST SRM 981 throughout the entire session match the accepted values of Galer and Abouchami [42]. The external precision was established to be 180 ppm (0.018% RSD) for all the ratios with ^{204}Pb and 40 ppm (0.004% RSD) for the other ratios.

Results

The Pb concentration and the Pb isotopic composition of the artefacts investigated are summarized in Tables 1, 2, 3. The Pb concentration for the bones ranges between 23 and $340 \mu\text{g g}^{-1}$ (RSD $<5\%$) with an average of $129 \mu\text{g g}^{-1}$. As a comparison, the bone lead level for non-occupationally

exposed “modern” teenagers, obtained via X-ray fluorescence spectrometry, was found to range up to $14.23 \mu\text{g}$ lead per gram bone mineral, with an average of $4.0 \pm 4.4 \mu\text{g g}^{-1}$ [43, 44]. The soil Pb content ranges from 13 to $71 \mu\text{g g}^{-1}$ (RSD $<5\%$) with an average of $28 \mu\text{g g}^{-1}$, being a normal range for soil lead, although distinguishing background Pb levels from levels affected by anthropogenic activities is difficult. Mean lead levels for different soil types range from 10 to $67 \mu\text{g g}^{-1}$, with an average of $32 \mu\text{g g}^{-1}$ [45], while the Pb concentration in the upper continental crust equals $20 \mu\text{g g}^{-1}$ [46]. For every bone–soil pair, the Pb concentration in the bone is higher by a factor of 2 to 10 compared to the corresponding soil. One soil sample (14-152-202, Table 1) shows a very low Pb concentration ($2 \mu\text{g g}^{-1}$), while the corresponding bone sample contains $29 \mu\text{g g}^{-1}$ Pb, which is not the lowest Pb concentration found for the full set of bones. Due to the very small amount of soil 14-152-202 available ($\sim 10 \text{ mg}$), together with the very low Pb concentration, no reliable isotope ratio measurement could be performed on this sample. The bone–soil pair 6-99-128 (Tables 1 and 2), on the other hand, shows an exceptionally high lead concentration compared to the other samples. The reason for the high lead concentration displayed by this pair remains unclear, as no lead objects were found inside this grave. The garum Pb concentration reaches $670 \mu\text{g g}^{-1}$ (Table 3). The lead objects were assumed to be 100% lead.

Graphical representations of the $^{207}\text{Pb}/^{206}\text{Pb}$ ratio versus the $^{208}\text{Pb}/^{206}\text{Pb}$ ratio and the $^{206}\text{Pb}/^{204}\text{Pb}$ ratio versus the $^{208}\text{Pb}/^{204}\text{Pb}$ ratio are given in Figs. 2 and 3, respectively. Three groups can be distinguished:

- a compact group of lead objects with a $^{208}\text{Pb}/^{206}\text{Pb}$ ratio between 2.087 and 2.088;
- a group of soil samples covering a $^{208}\text{Pb}/^{206}\text{Pb}$ range between 2.059 and 2.081; and
- a group of bone samples, located in-between the groups of lead objects on one side, and soil samples on the other side, in a $^{208}\text{Pb}/^{206}\text{Pb}$ range of 2.067–2.085. The lead in the soils is more radiogenic than that in the bones, which is again more radiogenic than the lead of the objects. The bone–soil pair 6-99-128 is characterised by a Pb isotopic composition similar to that of the lead objects, as are the soil 59-41-41 and the bone 51-54-165. The garum is situated between the lead objects and the bone group, but closer to the lead objects group, at a $^{208}\text{Pb}/^{206}\text{Pb}$ ratio of 2.085.

The $^{208}\text{Pb}/^{206}\text{Pb}$ ratio for every bone–soil pair is presented in Fig. 4. It can be seen that most of the bone–soil pairs display a significantly different isotopic composition for bone and soil. The $^{208}\text{Pb}/^{206}\text{Pb}$ ratio is systematically higher for the bones than for the soils, except for

Table 1 Pb concentrations and Pb isotope ratios for soil samples from the cemetery of *Pretorium Agrippinae*

	[Pb] ^a ($\mu\text{g g}^{-1}$)	²⁰⁶ Pb/ ²⁰⁴ Pb		²⁰⁷ Pb/ ²⁰⁴ Pb		²⁰⁸ Pb/ ²⁰⁴ Pb		²⁰⁷ Pb/ ²⁰⁶ Pb		²⁰⁸ Pb/ ²⁰⁶ Pb		²⁰⁸ Pb/ ²⁰⁷ Pb	
		IR	2s	IR	2s	IR	2s	IR	2s	IR	2s	IR	2s
1-140-165	17	18.845	0.007	15.662	0.006	38.847	0.015	0.83110	0.00008	2.06141	0.00018	2.48040	0.00019
6-53-75	23	18.640	0.007	15.654	0.005	38.600	0.015	0.83979	0.00008	2.07081	0.00018	2.46588	0.00019
6-99-128	3800	18.385	0.007	15.624	0.005	38.380	0.015	0.84990	0.00009	2.08706	0.00019	2.45572	0.00019
6-100-146	24	18.756	0.007	15.663	0.006	38.743	0.015	0.83508	0.00008	2.06559	0.00018	2.47352	0.00019
6-130-190	44	18.724	0.007	15.659	0.005	38.700	0.015	0.83629	0.00008	2.06690	0.00018	2.47146	0.00019
6-133-196	22	18.677	0.007	15.659	0.005	38.692	0.015	0.83842	0.00008	2.07172	0.00018	2.47097	0.00019
6-147-235	39	18.647	0.007	15.655	0.005	38.665	0.015	0.83958	0.00008	2.07363	0.00018	2.46982	0.00019
6-265-328	17	18.834	0.007	15.654	0.006	38.782	0.015	0.83147	0.00008	2.05922	0.00018	2.47751	0.00019
14-116-188	71	18.589	0.007	15.663	0.006	38.689	0.015	0.84258	0.00009	2.08123	0.00019	2.47008	0.00019
14-120-193	29	18.710	0.007	15.656	0.006	38.726	0.015	0.83680	0.00008	2.06982	0.00018	2.47350	0.00019
14-152-202	2	n.d. ^b		n.d.		n.d.		n.d.		n.d.		n.d.	
14-173-242	24	18.684	0.007	15.658	0.005	38.687	0.015	0.83807	0.00008	2.07062	0.00018	2.47067	0.00019
51-54-165	27	18.628	0.007	15.656	0.005	38.679	0.015	0.84044	0.00008	2.07637	0.00018	2.47055	0.00019
51-60-176	20	18.784	0.007	15.665	0.006	38.772	0.015	0.83395	0.00008	2.06403	0.00018	2.47502	0.00019
59--169	13	18.704	0.007	15.656	0.005	38.756	0.015	0.83702	0.00008	2.07209	0.00018	2.47557	0.00019
59-41-41	25	18.386	0.007	15.646	0.005	38.424	0.015	0.85099	0.00009	2.08988	0.00019	2.45583	0.00019
59-43-63	20	18.795	0.007	15.648	0.005	38.739	0.015	0.83258	0.00008	2.06114	0.00018	2.47560	0.00019
59-76-110	38	18.719	0.007	15.655	0.006	38.689	0.015	0.83629	0.00008	2.06680	0.00018	2.47137	0.00019
59-96-204	24	18.715	0.007	15.643	0.005	38.670	0.015	0.83585	0.00008	2.06619	0.00018	2.47196	0.00019
71-26-45	26	18.581	0.007	15.644	0.005	38.588	0.015	0.84191	0.00008	2.07673	0.00018	2.46670	0.00019
71-29-54	23	18.718	0.007	15.661	0.006	38.748	0.015	0.83667	0.00008	2.07007	0.00018	2.47416	0.00019
73-53-79	22	18.600	0.007	15.648	0.005	38.572	0.015	0.84128	0.00008	2.07379	0.00018	2.46504	0.00019

^a Determined via quadrupole-based ICP–MS, typical uncertainty (RSD): <5%

^b Not determined (only 10 mg sample available)

six bone–soil pairs. Two of these six pairs (6-99-128 and 6-147-235) display the same ²⁰⁸Pb/²⁰⁶Pb ratio while the other four pairs (14-173-242, 59--169, 59-41-41 and 71-26-45) display a ²⁰⁸Pb/²⁰⁶Pb ratio that is higher for the soils than for the bones. The spread in ²⁰⁸Pb/²⁰⁶Pb ratio is lower for the bones than for the soils.

Discussion

Controversy exists concerning the origin of high lead concentrations as retrieved in bone tissue dating from the Roman—or in general, any historical—era. Martínez-García et al. [47] interpret Pb levels higher than biogenic ranges found in Roman bone tissue as the result of dietary uptake or uptake by inhalation, while Millard [48] and Zapata et al. [49] consider diagenesis as the most important process leading to these high Pb concentrations. In the samples studied here, it turned out that:

1. the Pb levels are 2 to 10 times higher in the bone compared to the surrounding soil; and
2. one soil (14-152-202) has a very low Pb concentration ($2 \mu\text{g g}^{-1}$) compared to a much higher Pb concentration of the corresponding bone ($29 \mu\text{g g}^{-1}$).

It seems unlikely that all the lead present in the soil has moved into the bone. From these observations, the importance of diagenesis as a cause of high bone-lead concentrations can already be questioned, and uptake from food appears to be more likely. However, this statement is only based on Pb concentrations, and, as suggested by Millard [48], isotope ratios can provide a more profound insight into the relative contribution of diagenesis.

The percentage shift in ²⁰⁸Pb/²⁰⁶Pb isotope ratio from soil to bone (Fig. 4) varies between -0.64% (bone–soil pair 59-41-41) and 0.84% (bone–soil pair 51-60-176). However, no systematic correlation is observed between, on the one hand, the magnitude of the ²⁰⁸Pb/²⁰⁶Pb isotope ratio shift, and on the other hand:

1. the place on the excavation site where the sample was taken (indicated by the first number in the sample identification code, as given in Tables 1 and 2); and
2. the absolute values of the ²⁰⁸Pb/²⁰⁶Pb isotope ratios for bone and soil.

Furthermore, no systematic trend could be discerned between the absolute difference between the ²⁰⁸Pb/²⁰⁶Pb isotope ratio for bone and the corresponding soil, on one hand, and the absolute difference in concentration between

Table 2 Pb concentrations and Pb isotope ratios for bone samples from the cemetery of *Pretorium Agrippinae*

	[Pb] ^a ($\mu\text{g g}^{-1}$)	²⁰⁶ Pb/ ²⁰⁴ Pb		²⁰⁷ Pb/ ²⁰⁴ Pb		²⁰⁸ Pb/ ²⁰⁴ Pb		²⁰⁷ Pb/ ²⁰⁶ Pb		²⁰⁸ Pb/ ²⁰⁶ Pb		²⁰⁸ Pb/ ²⁰⁷ Pb	
		IR	2s	IR	2s	IR	2s	IR	2s	IR	2s	IR	2s
1-140-165	110	18.581	0.007	15.665	0.006	38.616	0.015	0.84309	0.00009	2.07835	0.00018	2.46518	0.00019
6-53-75	79	18.630	0.007	15.659	0.005	38.631	0.015	0.84052	0.00008	2.07358	0.00018	2.46703	0.00019
6-99-128	32000	18.396	0.007	15.633	0.005	38.390	0.015	0.84980	0.00009	2.08685	0.00019	2.45569	0.00019
6-100-146	150	18.575	0.007	15.660	0.005	38.629	0.015	0.84306	0.00009	2.07959	0.00018	2.46671	0.00019
6-130-190	64	18.647	0.007	15.654	0.005	38.613	0.015	0.83952	0.00008	2.07071	0.00018	2.46655	0.00019
6-133-196	31	18.591	0.007	15.652	0.005	38.577	0.015	0.84195	0.00008	2.07508	0.00018	2.46460	0.00019
6-147-235	170	18.640	0.007	15.660	0.005	38.646	0.015	0.84017	0.00008	2.07336	0.00018	2.46778	0.00019
6-265-328	160	18.632	0.007	15.644	0.005	38.577	0.015	0.83965	0.00008	2.07053	0.00018	2.46593	0.00019
14-116-188	320	18.540	0.007	15.659	0.005	38.623	0.015	0.84459	0.00009	2.08316	0.00019	2.46646	0.00019
14-120-193	200	18.561	0.007	15.648	0.005	38.573	0.015	0.84301	0.00009	2.07812	0.00018	2.46512	0.00019
14-152-202	29	18.599	0.007	15.654	0.005	38.609	0.015	0.84164	0.00008	2.07570	0.00018	2.46625	0.00019
14-173-242	44	18.684	0.007	15.661	0.006	38.658	0.015	0.83818	0.00008	2.06897	0.00018	2.46842	0.00019
51-54-165	300	18.428	0.007	15.629	0.005	38.413	0.015	0.84813	0.00009	2.08453	0.00019	2.45781	0.00019
51-60-176	340	18.529	0.007	15.652	0.005	38.566	0.015	0.84477	0.00009	2.08148	0.00019	2.46397	0.00019
59--169	59	18.705	0.007	15.653	0.005	38.663	0.015	0.83688	0.00008	2.06696	0.00018	2.46983	0.00019
59-41-41	124	18.592	0.007	15.660	0.005	38.609	0.015	0.84230	0.00008	2.07666	0.00018	2.46544	0.00019
59-43-63	122	18.525	0.007	15.636	0.005	38.502	0.015	0.84407	0.00009	2.07841	0.00018	2.46238	0.00019
59-76-110	88	18.617	0.007	15.658	0.006	38.651	0.015	0.84104	0.00008	2.07607	0.00018	2.46847	0.00019
59-96-204	47	18.536	0.007	15.643	0.005	38.518	0.015	0.84394	0.00009	2.07812	0.00018	2.46239	0.00019
71-26-45	23	18.589	0.007	15.650	0.005	38.581	0.015	0.84190	0.00008	2.07542	0.00018	2.46515	0.00019
71-29-54	160	18.584	0.007	15.656	0.006	38.628	0.015	0.84244	0.00008	2.07852	0.00018	2.46727	0.00019
73-53-79	75	18.498	0.007	15.645	0.005	38.529	0.015	0.84568	0.00009	2.08272	0.00019	2.46276	0.00019

^a Determined via quadrupole-based ICP–MS, typical uncertainty (RSD): <5%

bone and corresponding soil, on the other hand. The apparent lack of a systematic correlation between the difference in ²⁰⁸Pb/²⁰⁶Pb isotope ratio and the difference in Pb concentration for bone and corresponding soil can be taken as a first argument in excluding the process of diagenesis as the most important source of bone lead.

The graphical representation of the ²⁰⁷Pb/²⁰⁶Pb ratio versus the ²⁰⁸Pb/²⁰⁶Pb ratio (Fig. 2) displays an alignment of the bones with the soils, garum, and lead objects. This

suggests that the bone lead is a mixture of lead from two sources:

1. soils, and
2. lead objects and/or garum

confirming that the process of diagenesis is not the only lead source for bone. Furthermore, owing to the high precision of the measurement, it could be deduced that at least one additional source is required for complete clarifi-

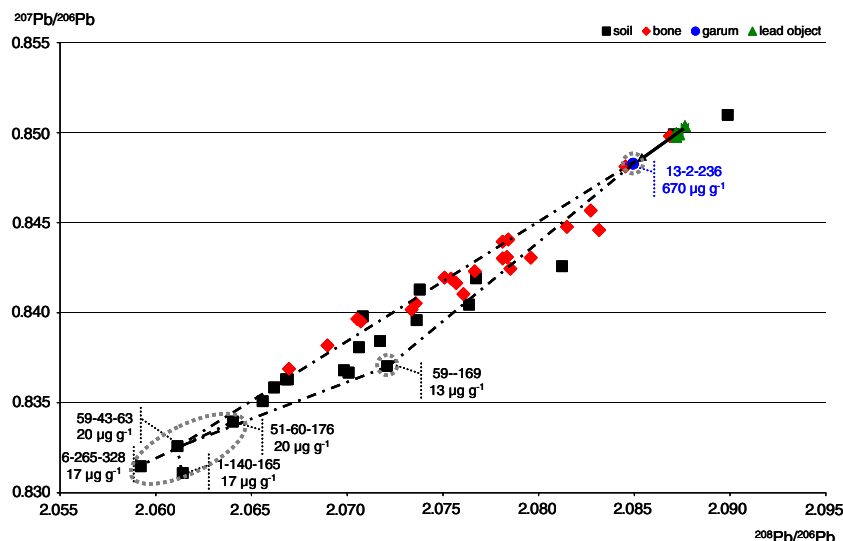
Table 3 Pb concentrations and Pb isotope ratios for garum and lead objects excavated around the cemetery of *Pretorium Agrippinae*

	[Pb] ^a ($\mu\text{g g}^{-1}$)	²⁰⁶ Pb/ ²⁰⁴ Pb		²⁰⁷ Pb/ ²⁰⁴ Pb		²⁰⁸ Pb/ ²⁰⁴ Pb		²⁰⁷ Pb/ ²⁰⁶ Pb		²⁰⁸ Pb/ ²⁰⁶ Pb		²⁰⁸ Pb/ ²⁰⁷ Pb	
		IR	2s	IR	2s	IR	2s	IR	2s	IR	2s	IR	2s
<i>Garum</i>													
13-2-236	670	18.435	0.007	15.638	0.005	38.436	0.015	0.84828	0.00009	2.08493	0.00019	2.45784	0.00019
<i>Lead objects</i>													
2-24-10	– ^b	18.388	0.007	15.630	0.005	38.378	0.015	0.84997	0.00009	2.08720	0.00019	2.45560	0.00019
5-67-499	– ^b	18.386	0.007	15.627	0.005	38.379	0.015	0.84991	0.00009	2.08734	0.00019	2.45598	0.00019
6-62-20	– ^b	18.395	0.007	15.624	0.005	38.394	0.015	0.84976	0.00009	2.08719	0.00019	2.45646	0.00019
7-547-971	– ^b	18.381	0.007	15.631	0.005	38.373	0.015	0.85036	0.00009	2.08764	0.00019	2.45506	0.00019
9-63-60	– ^b	18.382	0.007	15.624	0.005	38.367	0.015	0.84992	0.00009	2.08713	0.00019	2.45563	0.00019

^a Determined via quadrupole-based ICP–MS, typical uncertainty (RSD): <5%

^b Assumed to be 100% lead

Fig. 2 $^{207}\text{Pb}/^{206}\text{Pb}$ ratio versus $^{208}\text{Pb}/^{206}\text{Pb}$ ratio for the bone, garum, soil, and lead object samples investigated. Error bars ($2s$, external precision) are included in the symbol size. The endmembers identified are *encircled*. The code and Pb concentration of the samples considered as endmembers are indicated



cation. This assumption is confirmed in the representation of the $^{206}\text{Pb}/^{204}\text{Pb}$ ratio versus the $^{208}\text{Pb}/^{204}\text{Pb}$ ratio (Fig. 3), where the spread of the samples is wider.

The $^{208}\text{Pb}/^{206}\text{Pb}$ ratio was plotted versus the inverse of the Pb concentration (Fig. 5). From this graph, two soil endmembers can be clearly identified:

1. soil 59- -169, and
2. a group consisting of four soils: 1-140-165, 6-265-328, 51-60-176, and 59-43-63.

The first endmember, soil 59- -169, displays a $^{208}\text{Pb}/^{206}\text{Pb}$ ratio of 2.072 and a Pb concentration of $13 \mu\text{g g}^{-1}$, being the lowest Pb concentration after the abnormally low Pb concentration for soil 14-152-202 ($2 \mu\text{g g}^{-1}$) (Table 1). This soil can be considered as a representation of the local soil, largely free of Pb contamination. The second endmember

consists of the group of four soils mentioned above, all of which were excavated at a different place on the excavation site. The average isotopic composition for this four-soil group equals 18.8 for $^{206}\text{Pb}/^{204}\text{Pb}$, 15.65 for $^{207}\text{Pb}/^{204}\text{Pb}$, 38.8 for $^{208}\text{Pb}/^{204}\text{Pb}$, 0.83 for $^{207}\text{Pb}/^{206}\text{Pb}$, and 2.06 for $^{208}\text{Pb}/^{206}\text{Pb}$, which is in agreement with the range of Pb isotope ratio values given for the earth's crust [50, 51]. Furthermore, these four soils display Pb concentrations between 17 and $20 \mu\text{g g}^{-1}$, which is in the range of the Pb concentration of the upper continental crust [46]. As a consequence, this endmember may represent the earth's crust, rather than a second local background.

Next to soil, the group of lead objects can be considered as a lead source (Figs. 2 and 3). For the garum it was observed that:

1. its isotopic composition approaches that of the Pb from the objects (Table 3); and

Fig. 3 $^{206}\text{Pb}/^{204}\text{Pb}$ ratio versus $^{208}\text{Pb}/^{204}\text{Pb}$ ratio for the bone, garum, soil, and lead object samples investigated. Error bars represent $2s$ intervals (external precision). The endmembers identified are *encircled*. The code and Pb concentration of the samples considered as endmembers are indicated

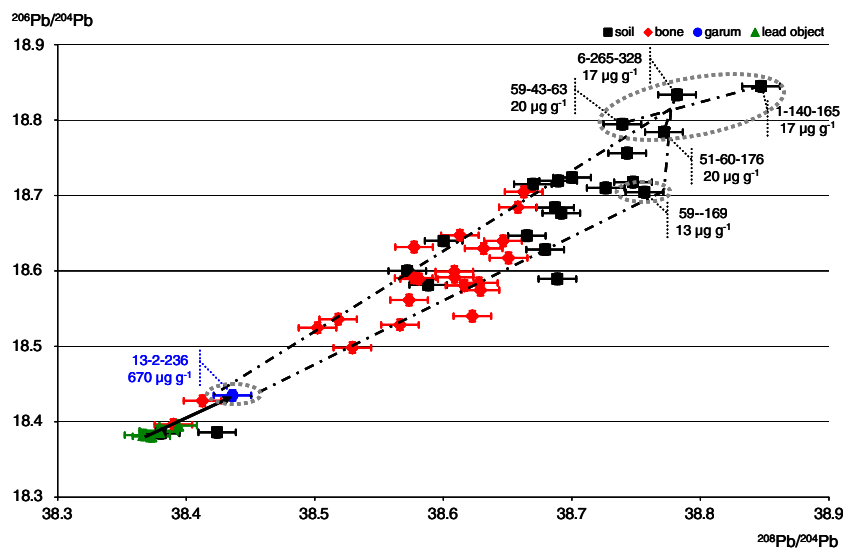
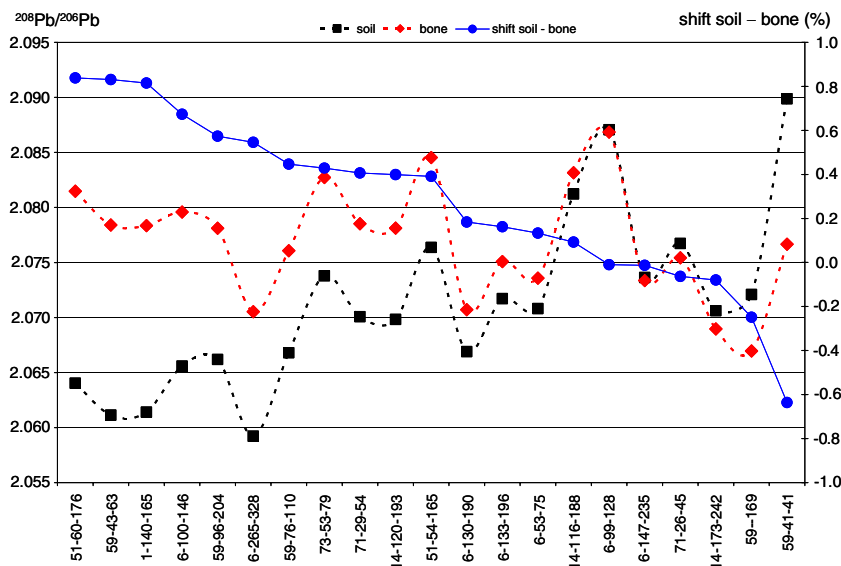


Fig. 4 $^{208}\text{Pb}/^{206}\text{Pb}$ ratio for bone–soil pairs, organised according to decreasing difference (%) between $^{208}\text{Pb}/^{206}\text{Pb}$ ratios for the soil and the bone. Error bars on the isotope ratios ($2s$, external precision) are included in the symbol size



2. its Pb concentration amounts to $670 \mu\text{g g}^{-1}$ (Table 3), a concentration that is twice as high as the highest bone lead concentration, found for sample 51-60-176 (6-99-128 excluded) (Table 2).

From this observation, the garum can be considered as contaminated with Pb coming from the lead objects, and thus represents a proxy for the lead objects. Since the garum was ingested by the Romans as a fish sauce, it makes more sense to consider garum and/or lead coming from the lead objects (via, e.g., drinking water) as a source of bone lead, rather than the Pb objects themselves. The observation that a higher bone Pb concentration (lower $1/\text{Pb}$ value) is characterised by an isotopic composition approaching that of garum and lead objects, confirms the assumption of garum,

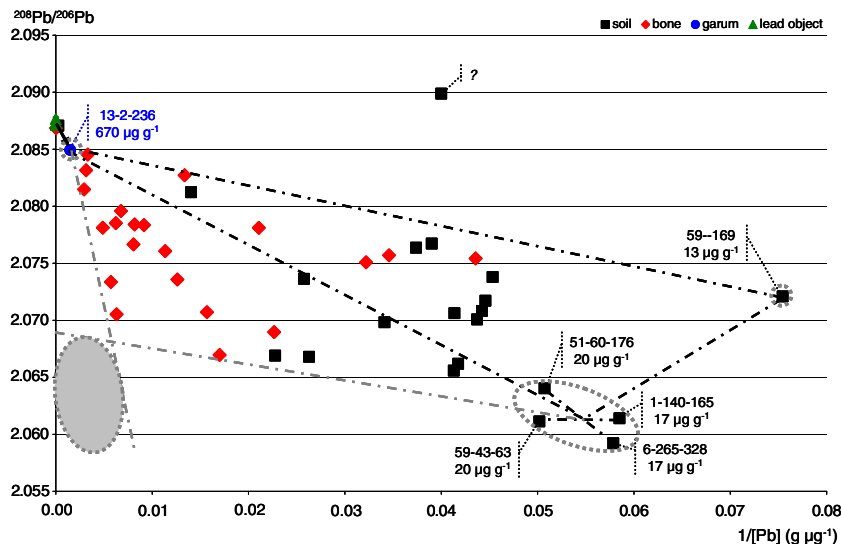
in its turn contaminated by Pb coming from the objects, as a third endmember.

As a conclusion, soil and lead objects were established as sources of bone lead. Three endmembers have been identified so far:

1. soil 59--169 as the local soil background;
2. a group of four soils (1-140-165, 6-265-328, 51-60-176 and 59-43-63) representative of the earth’s crust; and
3. garum, which in its turn was contaminated with Pb from the lead objects.

In Figs. 2, 3 and 5, the endmembers identified so far, have been indicated. However, with these endmembers only, not all the bone samples occur in the three-point diagrams constructed. This implies that at least one additional

Fig. 5 $^{208}\text{Pb}/^{206}\text{Pb}$ ratio versus the inverse of the Pb concentration. Error bars ($2s$, external precision) are included in the symbol size. The endmembers identified are *encircled*. The area indicated in *grey* indicates the expected position of a remaining endmember. One soil (59-41-41) is clearly out of the range for the other samples, and remains unexplained



endmember remains to be identified, which should have a $^{208}\text{Pb}/^{206}\text{Pb}$ ratio not higher than 2.067 (Fig. 5).

Four samples (bone and soil 6-99-128, bone 51-54-165, and soil 59-41-41) have an isotopic composition that is between that of the lead objects and that of the garum (Figs. 2 and 3). Both the bone tissue and the soil for sample set 6-99-128 show a very high lead concentration and an isotopic composition clearly deviating from that of the other bone–soil pairs (Tables 1 and 2), indicating a very high degree of contamination with lead from the lead objects. In Fig. 5 the soil 59-41-41 is located far from the range displayed by the other samples. For the moment, the reason why the soil 59-41-41 displays an isotopic composition clearly different from that of the other soil samples, remains unexplained.

From the considerations given above, it can be concluded that the process of diagenesis is not the most important source of lead found in the bones of Roman infants from *Pretorium Agrippinae*. The bone lead appears to be a mixture of geogenic lead (soil lead) and dietary exposure lead, taken up from, e.g., garum and/or drinking water.

Conclusions

Pb isotopic investigation of infant bone tissue dating from the Roman era, along with possible sources of bone lead such as surrounding soil, garum, and lead objects, has allowed determination of three endmembers for bone lead. Two endmembers were identified as soils, and the third endmember was shown to be lead coming from the lead objects, well represented by the fish bones used by the Romans to prepare garum, a fish sauce. These three endmembers however, do not completely explain the Pb isotopic composition of the full set of bone samples investigated, so that at least one additional endmember remains to be identified.

The studies conducted have revealed that the surrounding soil—and thus the process of diagenesis—can be excluded as the main source of bone lead. At least an important fraction of the lead retrieved in the bone tissue must have been present there before the decease of the infants whose remains have been retrieved at the cemetery of *Pretorium Agrippinae*.

More samples should be analysed, in order to identify the missing endmember(s). Further studies may be carried out to obtain insight into the toxicological aspect of this research, and to allow a more in-depth interpretation from an archaeological point of view concerning the sources of the lead found in the bone tissue investigated in this work.

Acknowledgements D.D.M. thanks the Special Research Fund (Bijzonder Onderzoeksfonds) from Ghent University for financial

support (grant B/05608/01). F.V. acknowledges the Fund for Scientific Research–Flanders (FWO-Vlaanderen) for financial support in the form of research projects 3G058506 and 3G066906.

References

1. Walczyk T (2004) *Anal Bioanal Chem* 378:229–231
2. Houk RS, Fassel VA, Flesch GD, Svec HJ, Gray AL, Taylor CE (1980) *Anal Chem* 52:2283–2289
3. Gray AL (1986) *J Anal At Spectrom* 1:403–405
4. Walder AJ, Freedman PA (1992) *J Anal At Spectrom* 7:571–575
5. Walder AJ, Furata N (1993) *Anal Sci* 9:675–680
6. Halliday AN, Lee DC, Christensen JN, Walder AJ, Freedman PA, Jones CE, Hall CM, Yi W, Teagle D (1995) *Int J Mass Spectrom Ion Proc* 146/147:21–33
7. Halliday AN, Lee DC, Christensen JN, Rehkämper M, Yi W, Luo X, Hall CM, Ballentine CJ, Pettke T, Stirling C (1998) *Geochim Cosmochim Acta* 62:919–940
8. Vanhaecke F, Moens L (2004) *Anal Bioanal Chem* 378:232–240
9. Ingle CP, Sharp BL, Horstwood MSA, Parrish RR, Lewis DJ (2003) *J Anal At Spectrom* 18:219–229
10. Archer C, Vance D (2004) *J Anal At Spectrom* 19:656–665
11. Wombacher F, Rehkämper M (2003) *J Anal At Spectrom* 18:1371–1375
12. Albarède F, Telouk P, Blichert-Toft J, Boyet M, Agranier A, Nelson B (2004) *Geochim Cosmochim Acta* 68:2725–2744
13. Rehkämper M, Mezger K (2000) *J Anal At Spectrom* 15:1451–1460
14. Albarède F, Beard B (2004) Analytical methods for non-traditional isotopes. In: Johnson CM, Beard BL, Albarède F (eds) *Reviews in mineralogy and geochemistry*, vol. 55, *Geochemistry of non-traditional stable isotopes*. Mineralogical Society of America, Washington
15. Philip AT, Gerson B (1994) *Clin Lab Med* 14:423–444
16. Gidlow DA (2004) *Occup Med-Oxford* 54:76–81
17. Piomelli S (2002) *Pediatr Clin N Am* 49:1285–1304
18. Hu H (1991) *Am J Public Health* 81:1070–1072
19. Philip AT, Gerson B (1994) *Clin Lab Med* 14:651–670
20. International Agency for Research on Cancer (1987) *Monographs on the evaluation of the carcinogenic risk of chemicals to humans* suppl 6:230–232
21. Papanikolaou NC, Hatzidaki EG, Belivanis S, Tzanakakis GN, Tsatsakis AM (2005) *Med Sci Monit* 11:329–336
22. Rabinowitz MB (1991) *Environ Health Perspect* 91:33–37
23. Rabinowitz MB, Wetherill GW, Kopple JD (1976) *J Clin Invest* 58:260–270
24. Rosman KJR, Taylor PDP (1998) *Pure Appl Chem* 70:217–235
25. Bouvier A, Blichert-Toft J, Moynier F, Vervoort JD, Albarède F (2007) *Geochim Cosmochim Acta* 71:1583–1604
26. Cloquet C, Carignan J, Libourel G (2006) *Atmos Environ* 40:574–587
27. Dolgoplova A, Weiss DJ, Seltmann R, Kober B, Mason TFD, Coles B, Stanley CJ (2006) *Appl Geochem* 21:563–579
28. Reinhard KJ, Ghazi AM (1992) *Am J Phys Anthropol* 89:183–195
29. Bower NW, Getty SR, Smith CP, Simpson ZR, Hoffman JM (2005) *Int J Osteoarchaeol* 15:360–370
30. Bower NW, McCants SA, Custodio JM, Ketterer ME, Getty SR, Hoffman JM (2007) *Sci Total Environ* 372:463–473
31. Columella LJM (1976) *De Re Rustica*. In: Ahrens K (ed) *Über Landwirtschaft: ein Lehr- und Handbuch der gesamten Acker- und Viehwirtschaft aus dem 1. Jahrhundert u.Z.* Akad.-Verl., Berlin
32. Gilfillan SC (1965) *J Occup Med* 7:53–60

33. Nriagu JO (1983) *N Engl J Med* 308:660–663
34. Bult EJ, Hallewas DP (1986) Graven bij Valkenburg I: het archeologisch onderzoek in 1985. Delft
35. Bult EJ, Hallewas DP (1987) Graven bij Valkenburg II: het archeologisch onderzoek in 1986. Delft
36. Bult EJ, Hallewas DP (1990) Graven bij Valkenburg III: het archeologisch onderzoek in 1987 en 1988. Delft
37. Plinius NH (1947) *Naturalis Historia*. In Rackham H (ed) *Naturalis Historia*. Cambridge
38. Smits E (2006) *Leven en sterven langs de Limes*, PhD dissertation, University of Amsterdam
39. De Muynck D, Cloquet C, Vanhaecke F (2007) *J Anal At Spectrom* DOI [10.1039/b709461b](https://doi.org/10.1039/b709461b)
40. Belshaw NS, Freedman PA, O’Nions RK, Frank M, Guo Y (1998) *Int J Mass Spectrom* 181:51–58
41. White WM, Albarède F, Télouk P (2000) *Chem Geol* 167:257–270
42. Galer SJG, Abouchami W (1998) *Miner Mag* 62A:491–492
43. Hoppin JA, Aro A, Hu H, Ryan PB (1997) *Pediatrics* 100:365–370
44. Farias P, Hu H, Rubenstein E, Meneses-Gonzalez F, Fishbein E, Palazuelos E, Aro A, Hernandez-Avila M (1998) *Environ Health Perspect* 106:733–737
45. Kabata-Pendias A, Pendias H (1984) *Trace elements in soils and plants*. CRC Press, Florida
46. Taylor SR, McLennan SM (1995) *Rev Geophys* 33:241–265
47. Martínez-García MJ, Moreno JM, Moreno-Clavel J, Vergara N, García-Sánchez A, Guillamón A, Portí M, Moreno-Grau S (2005) *Sci Total Environ* 348:51–72
48. Millard A (2006) *Sci Total Environ* 354:295–297
49. Zapata J, Pérez-Sirvent C, Martínez-Sánchez MJ, Tovar P (2006) *Sci Total Environ* 369:357–368
50. Elbaz-Poulichet F, Holliger P, Huang WW, Martin JM (1984) *Nature* 308:409–411
51. Weiss D, Shotyk W, Kramers JD, Gloor M (1999) *Atmos Environ* 33:3751–3763